Nat. Hazards Earth Syst. Sci. Discuss., 1, 7333–7356, 2013
www.nat-hazards-earth-syst-sci-discuss.net/1/7333/2013/
doi:10.5194/nhessd-1-7333-2013

Natural Hazards and Earth System Sciences
Discussions
Open Access

Storm-surge prediction at the Tanshui estuary: development model for maximum storm surges

C.-P. Tsai[1], C.-Y. You[1], and C.-Y. Chen[2]

[1]Department of Civil Engineering, National Chung Hsing University, Kuo Kuang Rd., Taichung 402, Taiwan
[2]Department and Graduate School of Computer Science, National Pingtung University of Education, No. 4–18, Ming Shen Rd., Pingtung 90003, Taiwan

Received: 16 October 2013 – Accepted: 13 November 2013 – Published: 10 December 2013

Correspondence to: C.-Y. Chen (cyc@mail.npue.edu.tw)

Published by Copernicus Publications on behalf of the European Geosciences Union.

Abstract

This study applies artificial networks, including both the supervised multilayer perception neural network and the radial basis function neural network to the prediction of storm-surges at the Tanshui estuary in Taiwan. The optimum parameters for the prediction of the maximum storm-surges based on 22 previous sets of data are discussed. Two different neural network methods are adopted to build models for the prediction of storm surges and the importance of each factor is also discussed. The factors relevant to the maximum storm surges, including the pressure difference, maximum wind speed and wind direction at the Tanshui Estuary and the flow rate at the upstream station, are all investigated. These good results can further be applied to build a neural network model for prediction of storm surges with time series data.

1 Introduction

Storm surges are sudden rises of water levels that can occur during typhoons, leading to the risk of flooding in low-lying coastal areas. Generally, storm surges are predicted using numerical methods. For example, Kawahara et al. (1980), Westerink et al. (1992), Blainetal (1994), and Hsu et al. (1999) applied the finite element method, Yen and Chou (1979), Walton and Christensen (1980), Harper and Sobey (1983), and Hwang and Yao (1987) applied the finite difference method with nonlinear shallow water equations to simulate storm surges.

In recent years, neural network technology has become more and more mature. It has been widely applied to non-linear natural phenomena. For example, Grubert (1995) used feed-forward back-propagation neural networks to predict the flow rate at a river mouth. Deo and Naidu (1999) used neural networks to build a model for real-time wave prediction. The results show that these neural networks perform better than that of the AR model for wave prediction. Tsai and Lee (1999) used back-propagation neural networks for real-time tide prediction. The predictions were very accurate and parameter

NHESSD
1, 7333–7356, 2013

fitting was not required for that model. Tsai et al. (2002) used the neural network technique for forecasting and supplementing the time series of wave data using neighbor station wave records. Marzenna (2003) used neural networks to predict storm surges and compared the results obtained using different neural network topologies. Lee et al. (2004) used short-term observational data to predict long-term sea levels with a back-propagation neural network and obtained accurate results.

Tsai et al. (2005) used back-propagation neural networks for the training of a water level time series model with data from previous typhoons used as training data to predict later typhoons. The prediction results were very good. However, the model was only used to predict overall water levels during storms. Storm surge values obtained by deducting astronomical tides from the predicted overall water levels might not be the same as actual values. In practice, astronomical tides plus storm surges equal the overall water levels during storms. Currently, astronomical tides can be well predicted using the harmonic analysis method or other numerical methods. Moreover, the maximum storm surge plus the highest spring tide may provide the potential for coastal inundation. Thus, the focus of this study is on the maximum storm surges.

2 Mathematical formulations

2.1 Storm surge empirical formula

Storm surges are also called irregular weather water levels. Studies on storm surges at specific spots are more meaningful with higher practical values. Storm surges are also related to weather conditions (e.g., wind speed, wind direction, and minimum atmospheric pressure). Regarding maximum storm surge estimations, Cornner (1957) believed that a larger center of low pressure would lead to higher wind speeds at a station. The pressure can be used to estimate storm surges. Unoki and Isozaki (1966) also believed that maximum storm surges can be expressed in terms of pressure. They analyzed all the storm surge data in Japan to obtain an empirical formulation for predicting storm surges at estuaries by the open sea.

Horikawa (1978) referenced the analysis results of previous actual data from Japan and suggested that, in addition to pressure, other parameters such as wind speed should also be taken into consideration. Their empirical formula is as follows:

$$\zeta_{max} = A\Delta P + B(V_{max})^2 \cos\theta, \quad (1)$$

where ζ_{max} is the maximum storm surge, ΔP is the maximum pressure difference during the storm surge, V_{max} is the maximum wind speed during the typhoon, θ is the angle between the direction of the wind with the maximum wind speed and the tide-gauge station's normal line, and A and B are the empirical constants at the maximum storm surge.

2.2 Multi layer perception network

A multi layer perception (MLP) network is a supervised learning method. This type of topology contains one input layer, one or more hidden layers, and one output layer. Data is sent to the output layer from the input layer using the feedforward method. The formulas are listed below:

$$y_j = f\left(\text{net}_j\right), \quad (2)$$

$$\text{net}_j = \sum_i W_{ij} X_i - B_j, \quad (3)$$

where y_j is the output variable, W_{ij} is the weight between the jth neural layer and the ith neural layer, X_i is the input variable as a biomimetic neuron input signal, $f(\text{net}_j)$ is the transformation function as a biomimetic non-linear function of the neurons, B_j is the threshold (bias) for the jth neuron, and net_j is the consolidation function for the jth neuron.

A transformation function is usually an S curve called a sigmoid function which increases stability and can be written as:

$$y_j = f\left(\sum W_{ij}X_i - B_j\right) = \frac{1}{1+e^{-\left(\sum W_{ij}X_i - B_j\right)}}. \quad (4)$$

The MLP network learning method, like the back-propagation neural network, is based on iteration. However, it allows for more than one hidden layer, therefore it can handle rather complex functions. Furthermore, with optimized network algorithms, the time and number of iterations required can be reduced. Usually the number of layers and neurons are obtained using a trial and error method. The best topology can thus be found. With enough hidden layers and neurons, any continuous function can be approximated.

2.3 Radial basis function network

The topology of the radial basis function (RBF) network is similar to that of the MLP network. Basically, the most advantageous feature of the RBF network is its fast learning speed, making it suitable for application in real-time systems. Its output can be written as:

$$F\left(x'\right) = \sum_{j=1}^{N} w_j \phi_j\left(x'\right) + B_j, \quad (5)$$

where x' is the input vector $(x_1, \ldots, x_p)^T$, W_j is the weight from the jth layer to the output layer, B_j is the threshold (bias) for the jth neuron, ψ_j is the basis function of the jth layer, and $F(x)$ is the output function of the network. The transformation function for the neurons in the output layer is a linear function.

NHESSD
1, 7333–7356, 2013

A common basis function used for the RBF network is a Gaussian function, which can be written as:

$$\phi_j(x') = \exp\left(-\frac{\left\|x' - U_j\right\|^2}{2\sigma_j^2}\right), j = 1,2,3\ldots N, \quad (6)$$

where σ_j is the smoothing parameter (called the width in this study) of the jth neuron which controls the radial basis function, U_j is the center of the neurons in the jth radial basis function hidden layer, and $\left\|x' - U_j\right\|$ is the Euclidean distance between U_j and the input vector.

3 Maximum storm surge prediction model

According to Murty (1984), over the past century, an average of 3.5 typhoons has struck Taiwan per year. Storm surges are very likely to occur at estuaries in the northern areas of Taiwan, such as Tanshui which is bordered by the Taiwan Strait. Data from the station at the Tanshui Estuary were collected in order to explore these storm surges.

3.1 Data sources

This study used storm surge and weather data acquired during typhoons from the station at the Tanshui Estuary (the tide-gauge station outside the southern dock of the second fishing port by the Tanshui Estuary) from 1996–2001 and in 2005. Data for 22 typhoons were selected based on their paths and whether they had caused serious storm surges at the Tanshui Estuary. The data used are summarized in Table 1. Data from the Xiulang Station, a hydrological station 25 km downstream from the Tanshui Estuary operated the Water Resources Agency on the Tamsui River were used.

NHESSD
1, 7333–7356, 2013

3.2 Pre-processing of data and evaluation indexes

Before training a neural network, pre-processing of the input data is very important. Input data must be normalized as discussed below:

$$x_{new} = \left[D_{min} + \frac{x_{old} - x_{min}}{x_{max} - x_{min}} \times (D_{max} - D_{min}) \right], \tag{7}$$

where D_{min} and D_{max} represent the range of linear mapping, x_{max} and x_{min} are the maximum and minimum values in the series, and $x_{old}$and x_{new} are the series before and after transformation.

Generally, network performances can be efficiently shown by looking at the errors and correlations obtained using two separate statistical indexes, the root mean square errors (RMSE) and correlation coefficients (C.C.). Their definitions follow:

$$\mathrm{RMSE} = \sqrt{\frac{\sum_{k=1}^{n} (y_k - \hat{y}_k)^2}{n}}, \tag{8}$$

where n is the sample size, y_k is the observed value of the kth sample point, and $\hat{y}_k$ is the kth estimation.

$$\mathrm{C.C.} = \frac{\sum_{k=1}^{n} (y_k - \bar{y}_k)\left(\bar{\hat{y}}_k - \bar{y}_k\right)}{\sqrt{\sum_{k=1}^{n} (y_k - \bar{y}_k)^2 \sum_{k=1}^{n} \left(\bar{\hat{y}}_k - \bar{y}_k\right)^2}}, \tag{9}$$

where y_k is the observed value of the kth sample point, $\hat{y}_k$ is the kth estimation, $\bar{\hat{y}}_k$ is the average of the estimations, and $\bar{y}_k$ is the average of the observed values.

NHESSD
1, 7333–7356, 2013

Storm-surge prediction at the Tanshui estuary

C.-P. Tsai et al.

3.3 Topology presentation of neural networks

In this study, the topologies of neural networks are presented in the form of "$I_x H_y O_z$", where I_x represents the number of neurons (factors which influenced storm surges, such as pressure difference, wind speed, etc.) in the input layer, H_y represents the number of hidden layers, and O_z represents the number of output variables. The number of output neurons was 1 (z =1) because there was only one variable to be predicted, the storm surge.

3.4 Empirical formulation

To obtain the empirical formula for finding the maximum storm surge, the generalized least squares method was applied with data for the 22 selected typhoons being used for the regression analysis. The following empirical constants for the Tanshui Estuary were obtained: $A = 0.00952$ and $B = 0.0031$. The formula can be written as:

$$\zeta_{\max} = 0.00952\Delta P + 0.0031(V_{\max})^2 \cos\theta. \quad (10)$$

Equation (10) is applied to the data for the 22 typhoons and the results are summarized in Fig. 1. According to the graph, the estimations obtained with the storm surge empirical formula are mostly lower than the observed values. The reason could be that there was not enough data for empirical calculation of the storm surge, leading to poor precision. The correlation coefficient is 0.565, as shown in Fig. 2.

4 Empirical verification

Three models were used for discussion based on the pressure difference (ΔP), the wind field factor ($U = V_{\max}^2 \cos\theta$) at the Tanshui Estuary and the flow rate (Q) from the upstream Xiulang Station (make segmentation). Model A: $\zeta_{\max} = f\ (\Delta P)$

Model B: $\zeta_{\max} = f\ (\Delta P, U)$

Model C: $\zeta_{\max} = f\ (\Delta P, U, Q)$

4.1 MODEL A

In line with scholars such as Cornner et al. (1957) and Isozaki (1966) who believe that pressure differences can be used to estimate maximum storm surges, this study first utilizes the pressure difference as the only input variable to build a neural network model to predict the maximum storm surge. As can be seen in Table 2, in Model A, the best topologies for the MLP and RBF neural network models are $I_1H_7O_1$ and $I_1H_8O_1$, respectively. According to the storm surge predictions shown in Figs. 3 and 4, the MLP model could predict some of the maximum storm surges based on a single input variable.

According to Table 2, although there was not sufficient precision, when using the pressure difference as the only input variable, the performance of the neural network model was better than that of the empirical formula.

4.2 MODEL B

In Model A, the only input variable was the maximum pressure difference. Then after that, another input variable, the corresponding wind field factor, was added to predict maximum storm surges. According to Table 2, the best network topologies for the MLP and RBF neural network models were $I_2H_7O_1$ and $I_2H_{11}O_1$. According to the correlation coefficients in Figs. 5 and 6, the predictions for maximum storm surges in Model B, in which the maximum wind factor was considered, were better than those in Model A. The correlation coefficient for the MLP model was 0.983, and that of the RBF model was 0.935.

Figures 3, 4, 7, and 8 show the maximum storm surge predictions of Models A and B. According to these figures, the predictions obtained using both the MLP model and the RBF model in Model B were more precise than those in Model A. It is also found that the MLP predictions were more precise for typhoons causing larger storm surges. They were similar to the RBF predictions although not as precise as the MLP predictions. It

NHESSD
1, 7333–7356, 2013

Title Page
Abstract | Introduction
Conclusions | References
Tables | Figures
◀◀ | ▶▶
◀ | ▶
Back | Close
Full Screen / Esc
Printer-friendly Version
Interactive Discussion

is obvious that the influence of wind factor should not be ignored in the prediction of the maximum storm surge, especially for typhoons causing larger storm surges.

4.3 MODEL C – influences of upstream flow

The storm surges in estuaries can be categorized into those in estuaries near seas and in estuaries near rivers. The storm surges discussed in this study are the former. The maximum pressure difference and wind factor were used as inputs in Model B. In addition to the maximum pressure difference and the corresponding maximum wind speed, the upstream flow was input as well in Model C. According to Table 2, the best topologies for the MLP and RBF neural network models were $I_3H_6O_1$ and $I_3H_{10}O_1$, respectively.

According to the correlation coefficients in Table 2, the MLP and RBF models performed better for Model C (with upstream flow being input) than for Model B (without the input of upstream flow). However, the correlation for the MLP model in Model C were only 0.003 higher than that in Model B, while the correlation for the RBF model in Model C was lower than those in Model B.

Although according to the predictions of storm surges as shown in Figs. 7 and 9, the RMSE for the MLP model in Model B was slightly higher than that in Model C, while it can be seen from Figs. 8 and 10 that the RMSE for the RBF model was slightly lower for Model B than for Model C. Thus, it is likely that although the upstream flow had some influence on storm surge, the influence is far smaller than that of wind field and low pressure.

5 Conclusions

According to the results of Models A, B, and C, if the pressure difference was the sole input, Model A might be too dependent on one single factor to obtain precise predictions. In Model B, the factors used in Horikawa's (1978) formula were adopted,

NHESSD
1, 7333–7356, 2013

Title Page
Abstract Introduction
Conclusions References
Tables Figures
◀I ▶I
◀ ▶
Back Close
Full Screen / Esc
Printer-friendly Version
Interactive Discussion

where the wind field and maximum pressure difference were input. Neural network models can be used to predict highly non-linear influences, thereby improving on the disadvantages of the empirical formula. In Model C, although the upstream flow was a factor of influence on the storm surges, manual observations are required to obtain flow information during typhoons. However, it is very common for there to be missing values or large observation errors. Based on the above review and discussion, the best input factors for Model B would further be applied to build a neural network prediction of storm surges with time series.

Acknowledgements. The authors are appreciative of the support to the CYC and CPT received from the National Science Council of the Republic of China, under Grant No. NSC 99-2628-E-153-001 and No. NSC 96-2221-E-005-077-MY3. They are also most grateful for the kind assistance of the editor and for the constructive suggestions from the anonymous reviewers, all of which have led to the making of several corrections and have greatly aided us to improve the presentation of this paper.

References

Blain, C. A., Westerink, J. J., and Luettich, R. A., Jr.: The influence of domain size on the response characteristics of a hurricane storm surge model, J. Geophysical Res., 99, 18467–18479, 1994.

Conner, W. C., Kraft, R. H., and Lee, H. D.: Empirical methods for forecasting the maximum storm tide due to hurricanes and other tropical storms, Monthly Weather Review, 85, 113–116, 1957.

Deo, M. C. and Sridhar, N. C.: Real time wave forecasting using neural networks, Ocean Eng., 26, 191–203, 1999.

Grubert, J. P.: Prediction of estuarine instabilities with artificial neural networks, J. Comput. Civil Eng., 9, 266–274, 1995.

Harper, B. A. and Sobey, R. J.: Open-boundary conditions for open-coast hurricane storm surge, Coast. Eng. Japan, 7, 41–60, 1983.

Horikawa, K.: Coastal Engineering, Tokyo University Press, Tokyo, 153–167, 1978.

Hsu, T. W., Liao, J. M. and Lee, Z. S.: Prediction of storm surge at northestern coast of Taiwan by finite element method, J. Chinese Institute of Civil and Hydraulic Eng., 11, 849–857, 1999.
Hwang, R. R. and Yao, C. C.: A semi-implicit numerical model for storm surges, J. Chinese Instit. Engin., 10, 463–472, 1987.
Kawahara, M., Nakazawa, S., Ohmori, S., and Tagaki, T.: Two-step explicit finite element method for storm surge propagation analysis, Int. J. for Numerical Methods Eng., 15, 1129–1148, 1980.
Lee, T. L.: Back-propagation neural network for long-term tidal predictions, Ocean Eng., 31, 225–238, 2004.
Marzenna, S.: Forecast of storm surge by means of artificial neural network, J. Sea Res., 49, 317–322, 2003.
Murty, T. S.: Storm surges: Meteorological ocean tides, Canadian Bulletin of Fisheries and Aquatic Science (212), Dept. Fisheries Oc. Canada, 1984.
Tsai, C. P. and Lee, T. L.: Back-propagation neural network in tidal-level forecasting, J. Waterway, Port, Coastal and Ocean Eng., ASCE125, 195–202, 1999.
Tsai, C. P., Lin, C., and Shen, J. N.: Neural network for wave forecasting among multi-stations, Ocean Eng., 29, 1683–1695, 2002.
Tsai, C. P., Lee, T. L., Yang, T. J., and Hsu, Y. J.: Back-propagation neural networks for prediction of storm surge, Proceedings of the Eighth International Conference on the Application of Artificial Intelligence to Civil, Structural and Environmental Eng., Paper (45), Civil-comp Press, UK, 2005.
Unoki, S. and Isozaki, I.: A possibility of generation of surf beat, Proceedings of the 10th International Conference on Coastal Eng., ASCE, 1, 1207–1216, 1966.
Walton, R. and Christensen, B. A.: Friction factors in storm surges over inland areas, J. Waterway, Port, Coastal and Ocean Division, ASCE106, 261–271, 1980.
Westerink, J. J., Luettich, R. A., Baptista, A. M.,Scheffner, N. W., and Farrar, P.: Tide and storm surge predictions using a finite element model, J. Hrdraulic Eng., ASCE118, 1373–1390, 1992.
Yen, G. T. and Chou, F. K.: Moving boundary numerical surge model, J. Waterway, Port, Coastal and Ocean Division, ASCE105, 247–263, 1979.

Table 1. Maximum storm surge data.

Typhoon	ζ_{max} (m)	V_{max} (m s^{-1})	P(mb)	cosθ
(LOMGWANG)	0.135	8.1	16.55	−0.00175
(TALIM)	0.369	8.9	39.25	−0.64279
(HAITANE)	0.294	8.1	38.55	−0.00175
(MATSA)	0.561	8.6	26.55	−0.98481
(LEKIMA)	0.305	5.3	20.65	0.50000
(NARI)	0.220	7.1	16.15	0.76604
(TORAJI)	0.165	5.1	20.15	−0.34202
(CHEBI)	0.227	7.1	19.35	−0.76604
(XANGSANE)	0.881	9.1	14.55	0.98481
(BILIS)	0.290	8.8	24.75	−0.64279
(PRAPIROON)	0.588	5.2	22.95	0.50000
(KAI–TAI)	0.425	6.7	28.25	0.34202
(DAN)	0.435	7.1	12.65	−0.34202
(BABS)	0.247	3.6	7.15	0.92388
(ZEB)	0.799	11.7	30.75	0.70711
(YANNI)	0.183	5.4	15.25	1.00000
(OTTO)	0.191	6.3	18.65	−0.70711
(IVAN)	0.523	2.8	8.75	0.70711
(AMBER)	0.240	7.6	24.65	−0.70711
(WINNIE)	0.925	11.7	32.85	0.00000
(HERB)	0.953	9.9	47.75	1.00000
(GLORIA)	0.201	7.6	25.65	−0.70711

NHESSD

1, 7333–7356, 2013

Storm-surge prediction at the Tanshui estuary

C.-P. Tsai et al.

Table 2. Comparison of models for the prediction of storm surges.

Prediction Model $I_xH_yO_z$		Topologies evaluation indexes	Performance	Test	Input variable
Empirical Formula		–	RMSE	0.267	$\Delta P, U$
			C.C.	0.565	
Model A	MLP	$I_1H_7O_1$	RMSE	0.156	ΔP
			C.C.	0.801	
Model A	RBF	$I_1H_8O_1$	RMSE	0.172	ΔP
			C.C.	0.752	
Model B	MLP	$I_2H_7O_1$	RMSE	0.048	$\Delta P, U$
			C.C.	0.983	
Model B	RBF	$I_2H_{11}O_1$	RMSE	0.094	$\Delta P, U$
			C.C.	0.935	
Model C	MLP	$I_3H_6O_1$	RMSE	0.038	$\Delta P, U, Q$
			C.C.	0.985	
Model C	RBF	$I_3H_{10}O_1$	RMSE	0.110	$\Delta P, U, Q$
			C.C.	0.906	

NHESSD
1, 7333–7356, 2013

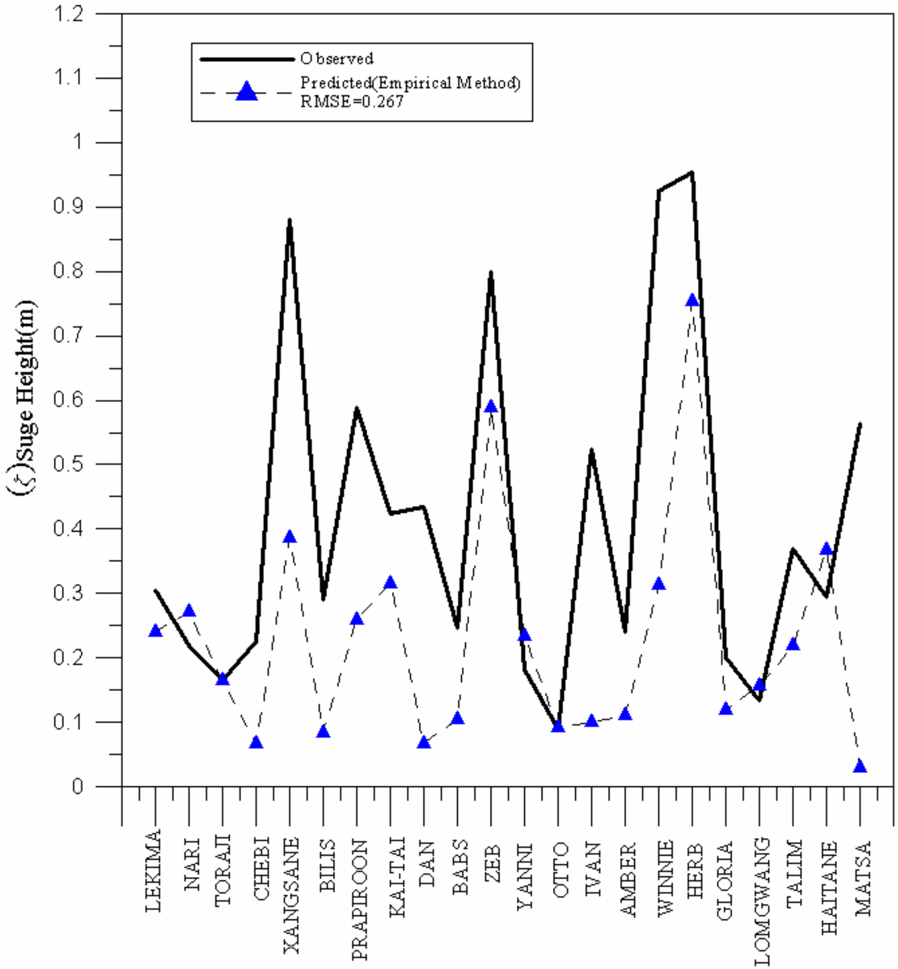

Fig. 1. Predictions obtained by the storm surge empirical formula.

NHESSD
1, 7333–7356, 2013

Storm-surge prediction at the Tanshui estuary

C.-P. Tsai et al.

Title Page
Abstract
Introduction
Conclusions
References
Tables
Figures
◀I
▶I
◀
▶
Back
Close
Full Screen / Esc
Printer-friendly Version
Interactive Discussion

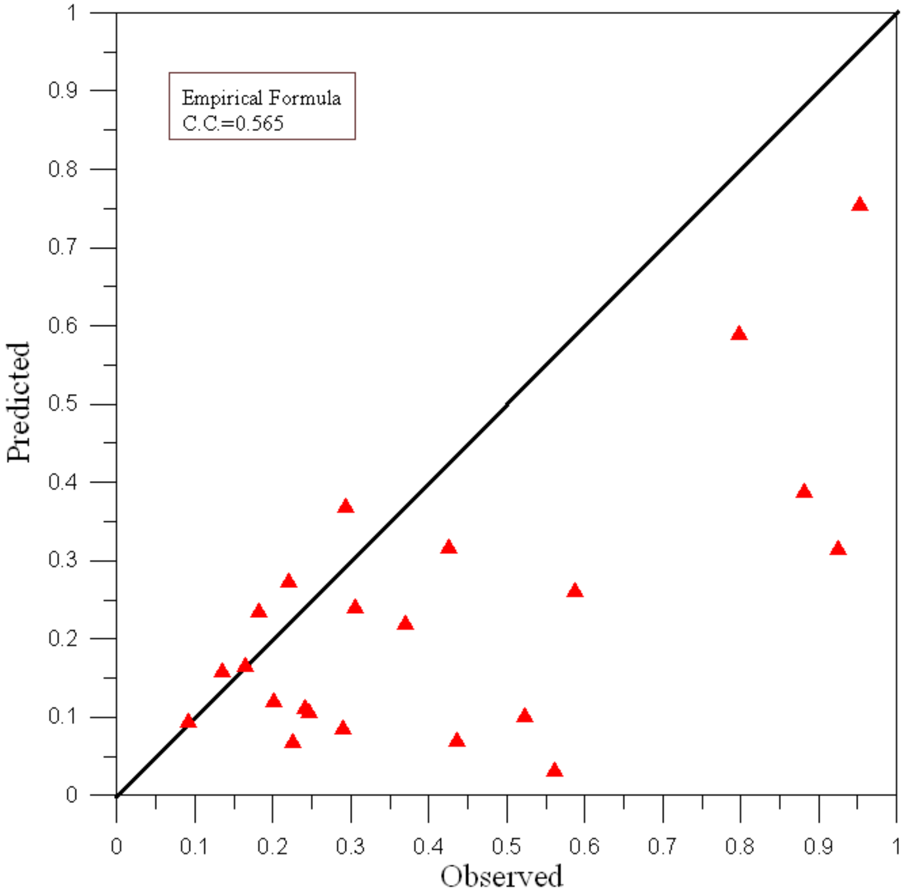

Fig. 2. Correlation coefficients from the storm surge empirical formula.

NHESSD
1, 7333–7356, 2013

Storm-surge prediction at the Tanshui estuary

C.-P. Tsai et al.

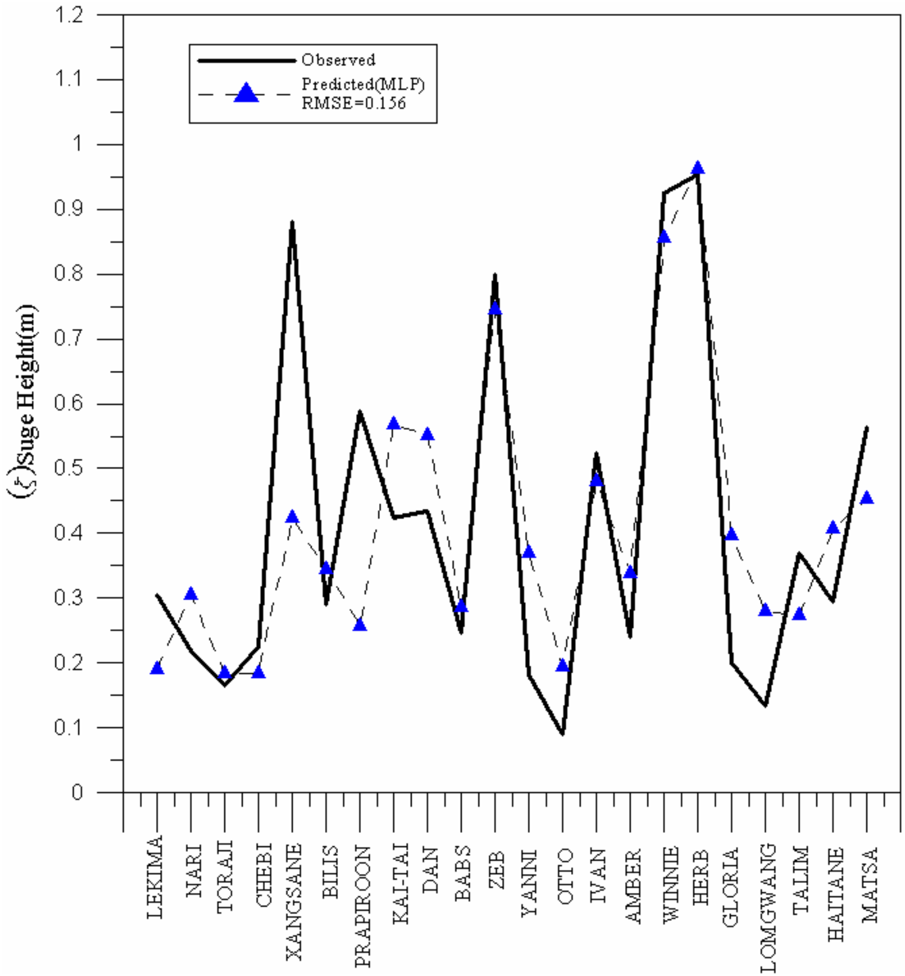

Fig. 3. MLP predictions of maximum storm surges (Model A).

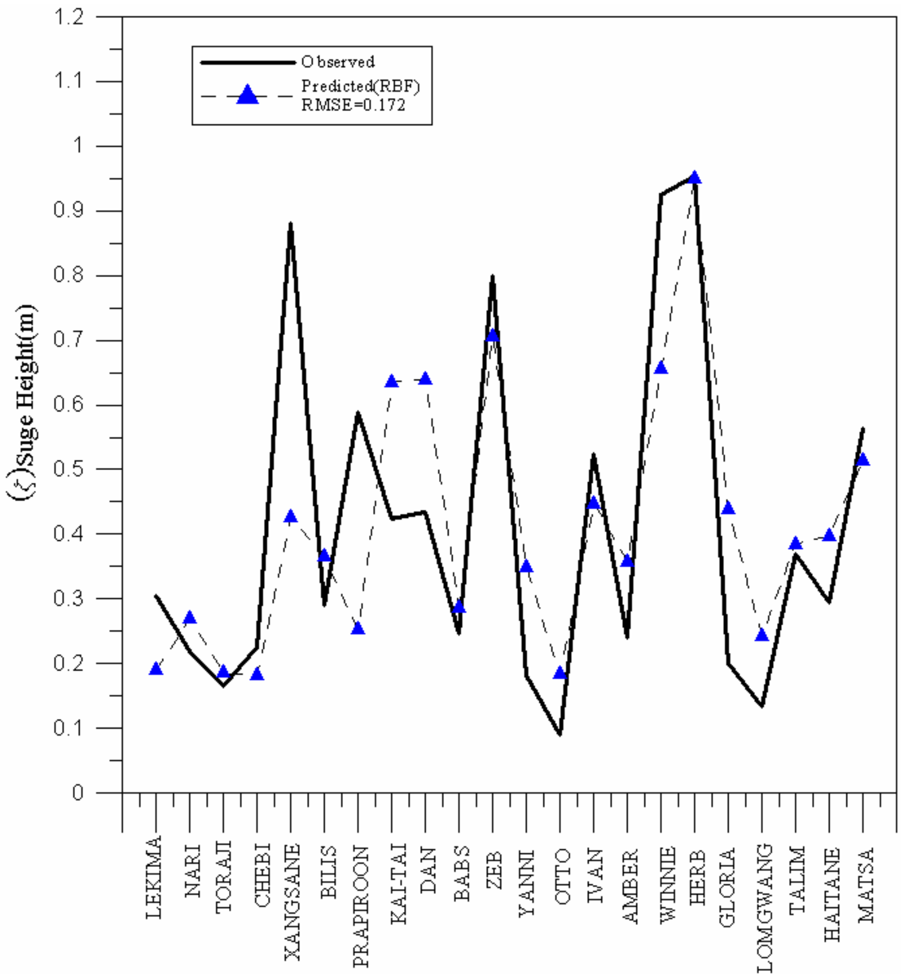

Fig. 4. RBF predictions of maximum storm surges (Model A).

NHESSD
1, 7333–7356, 2013

Storm-surge prediction at the Tanshui estuary

C.-P. Tsai et al.

Title Page
Abstract
Introduction
Conclusions
References
Tables
Figures
◀I
▶I
◀
▶
Back
Close
Full Screen / Esc
Printer-friendly Version
Interactive Discussion

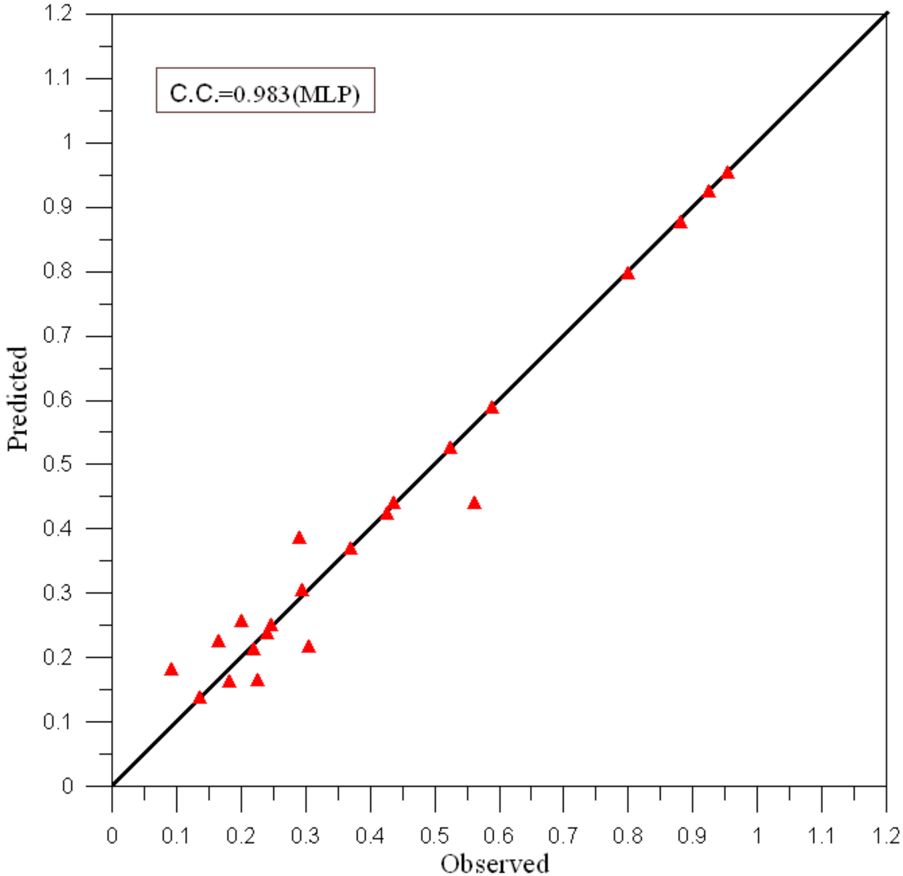

Fig. 5. Correlation coefficients of the MLP maximum storm surge predictions and observed values (Model B).

NHESSD
1, 7333–7356, 2013

Storm-surge prediction at the Tanshui estuary

C.-P. Tsai et al.

Title Page
Abstract | Introduction
Conclusions | References
Tables | Figures
◀| |▶
◀ ▶
Back | Close
Full Screen / Esc
Printer-friendly Version
Interactive Discussion

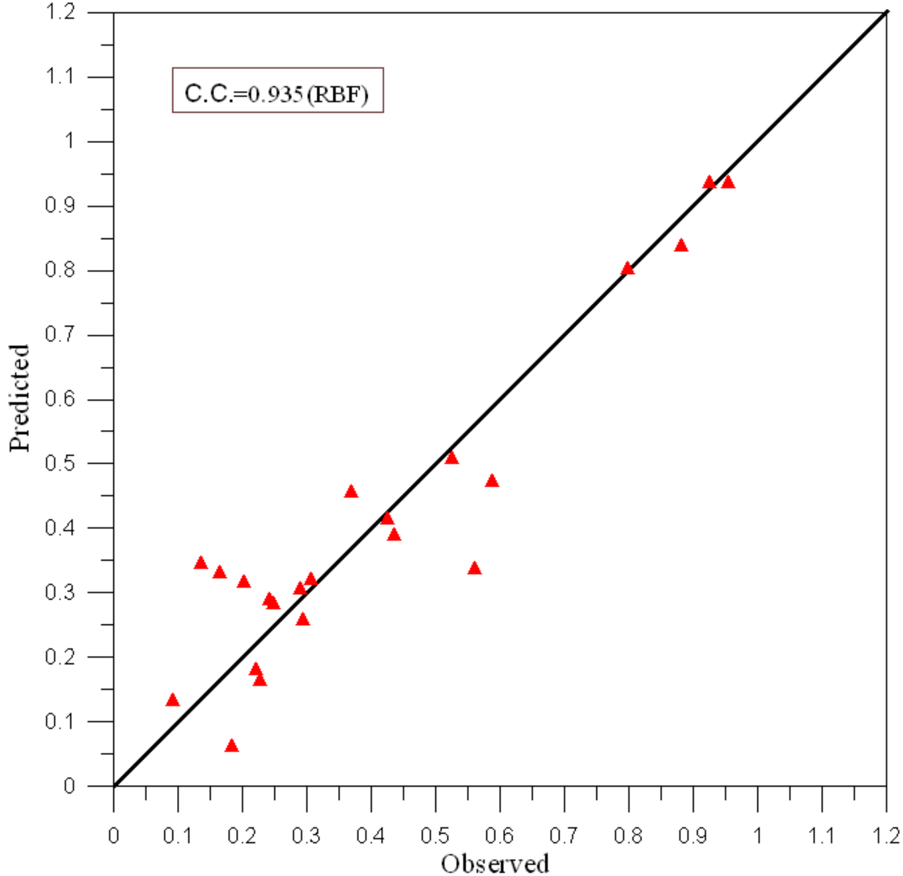

Fig. 6. Correlation coefficients of the RBF maximum storm surge predictions and observed values (Model B).

NHESSD
1, 7333–7356, 2013

Storm-surge prediction at the Tanshui estuary

C.-P. Tsai et al.

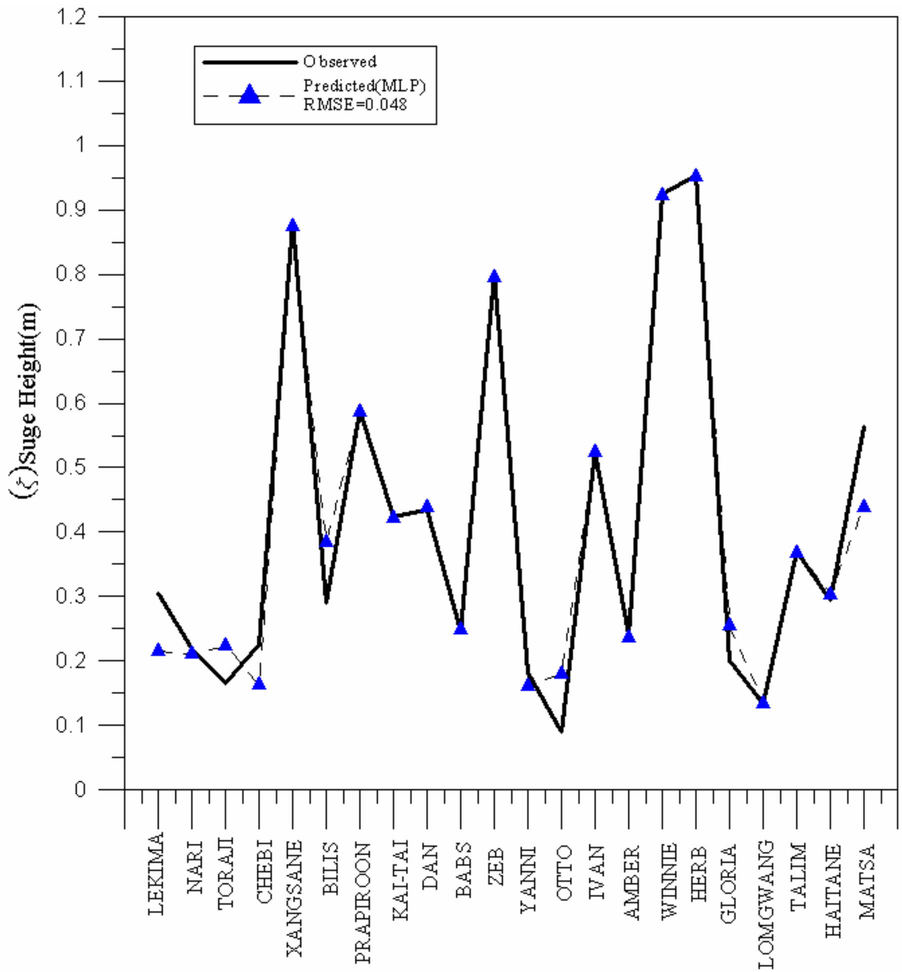

Fig. 7. Predictions of maximum storm surge using the MLP model (Model B).

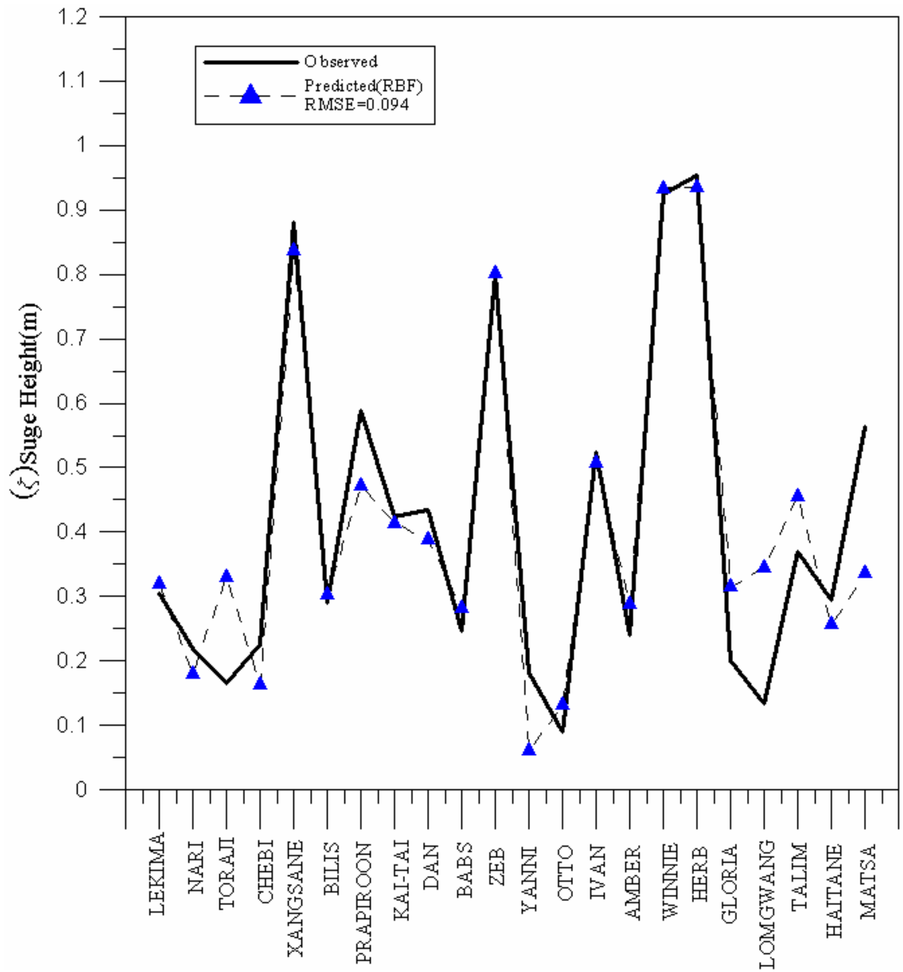

Fig. 8. Predictions of maximum storm surge using the RBF model (Model B).

NHESSD
1, 7333–7356, 2013

Storm-surge prediction at the Tanshui estuary

C.-P. Tsai et al.

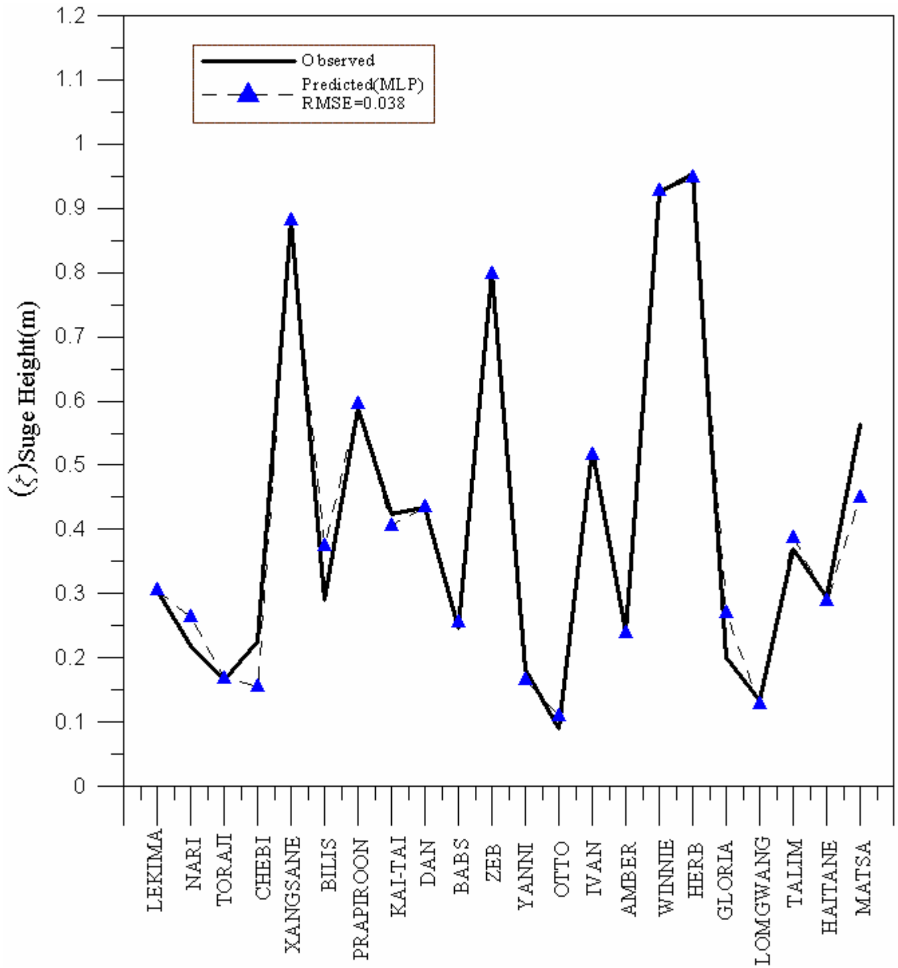

Fig. 9. Predictions of maximum storm surge using the MLP model (Model C).

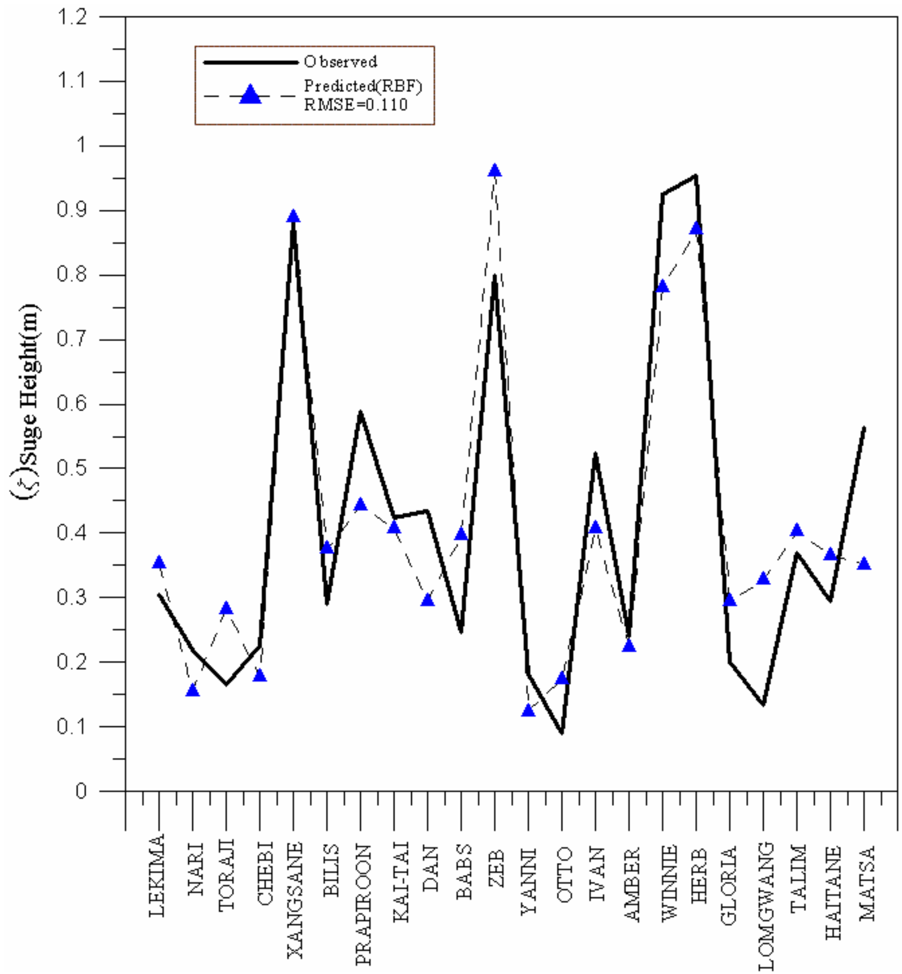

Fig. 10. Predictions of maximum storm surge using the RBF model (Model C).